

# International Conference on Space Optics—ICSO 2018

Chania, Greece

9–12 October 2018

*Edited by Zoran Sodnik, Nikos Karafolas, and Bruno Cugny*



## *Type-II superlattices: a promising material for space applications*

*V. Daumer*

*F. Rutz*

*A. Wörl*

*J. Niemasz*

*et al.*



ics0 proceedings



# Type-II superlattices – a promising material for space applications

V. Daumer\*, F. Rutz, A. Wörl, J. Niemasz, R. Müller, T. Stadelmann, and R. Rehm  
Fraunhofer Institute for Applied Solid State Physics IAF, Tullastr. 72, D-79108 Freiburg, Germany

## ABSTRACT

Type-II superlattices (T2SLs) are currently recognized as the sole material system offering comparable performance to HgCdTe, yet providing higher operability, stability over time, spatial uniformity, scalability to larger formats, producibility and affordability. Hence, T2SL technology is very promising for space applications. Fraunhofer IAF played a vital role in the development of III-As/Sb T2SLs right from the beginning. Mono- and bi-spectral focal plane arrays up to 640×512 pixels for the mid- and long-wavelength infrared (IR) have been demonstrated. The growth of T2SL is performed by molecular beam epitaxy (MBE) in multi-wafer reactors. We report on the excellent homogeneity and reproducibility of the growth process, established in the past years at Fraunhofer IAF. After processing this material to detector arrays, the T2SL detectors have been characterized down to low temperatures (below 40K) with promising properties regarding the dark current. For MWIR and LWIR detectors the resolution limit of the measurement setup with a dark current density of  $2 \times 10^{-10}$  A/cm<sup>2</sup> has been reached at 77 K and 36 K, respectively.

**Keywords:** MWIR, LWIR, InAs/GaSb, type-II superlattice, T2SL, molecular beam epitaxy, MBE

## 1. INTRODUCTION

Antimony-based type-II superlattices (T2SLs) have reached market maturity in recent years and now start replacing HgCdTe detectors in first applications. The effective bandgap of T2SL can be tailored from mid wavelength infrared (MWIR, 3-5  $\mu\text{m}$ ) up to the long (LWIR, 8-12  $\mu\text{m}$ ) or even very-long wavelength infrared regime (VLWIR, >12 $\mu\text{m}$ ) when grown lattice-matched on GaSb substrates, which are already available up to 6 inch (6") in diameter. In one and the same optimized molecular epitaxial growth process the effective bandgap can be engineered by just selecting the appropriate thickness for the alternating InAs and GaSb layers, which offers the possibility to design heterojunction devices including unipolar barrier layers with higher bandgap to reduce the dark current. While T2SLs provide quantum efficiency and responsivity comparable to HgCdTe, they excel in operability, stability over time, spatial uniformity, scalability to larger formats, producibility and affordability. In the frame of the US research and development program VISTA (Vital Infrared Sensor Technology Acceleration), for example, T2SL megapixel arrays for (V)LWIR have been demonstrated with dark currents below the heuristic trend line »Rule '07«<sup>1</sup> for HgCdTe detectors, recently. At low operating temperatures modern InAs/GaSb T2SL devices exhibit reduced tunneling current contributions to the dark current compared to HgCdTe due to a much higher effective electron mass and the use of heterojunction concepts. In summary, this emerging material system offers comparable performance and benefits from mature III/V process technology.

## 2. MATURING OF T2SL TECHNOLOGY

To provide an industry-compatible T2SL technology, Fraunhofer IAF has established the complete chain for detector array fabrication including design and modelling, epitaxial growth, as well as front- and backside processing. For the design of complex heterostructures we have extended the two-component superlattice empirical pseudopotential method (SEPM) by the inclusion of InSb-like interface layers, which are necessary for the growth of InAs/GaSb SLs to compensate for the resulting strain. Furthermore, the inclusion of arsenic from the background of the MBE chamber in the nominal As-free GaSb layers has been taken into account for the calculations. This four-component SEPM and the good agreement with the experimental results are described elsewhere<sup>2</sup>.

The epitaxial growth described in this chapter is performed in a VEECO GEN200 MBE reactor in a 5×3" platen configuration with a 2" witness wafer in the center. The MBE is equipped with SUMO™ sources for In, Ga and Al, valved cracker

\*volker.daumer@iaf.fraunhofer.de; phone +49 761 5159-867; fax +49 761 5159-71867; www.iaf.fraunhofer.de

cells for As and Sb, and dopant cells for Si, Be and GaTe. Amongst other projects, this MBE is one of the material sources for our pilot line production of dual-color detector arrays, used in a procurement program which is at TRL8 on the system level. The growth structure consists of layers that form two back-to-back photodiodes with two different bandgaps, which are engineered to detect the strong CO<sub>2</sub> signature around 4.25 μm. By coincident and simultaneous operation of the two photodiodes, the detector discriminates hot CO<sub>2</sub> from, e.g., a missile plume against a broad spectrum IR background with sun reflections and clutter. This reduces the false alarm rate in missile warning applications in contrast to mono-spectral detectors dramatically. The bandgap of the two photodiodes can be deduced from low temperature photoluminescence (PL) measurements. The photodiodes are labeled “red” and “blue” for the longer and shorter cut-off wavelength above and below the CO<sub>2</sub> signature, respectively.

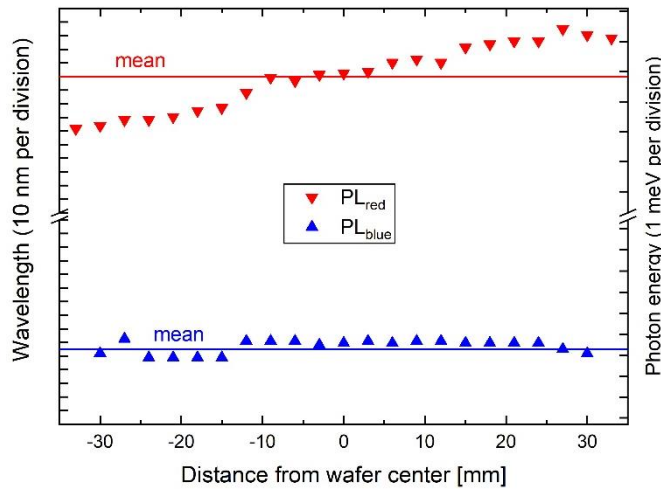


Figure 1. PL peak positions at different distances from the center of a 3” wafer in a 5×3” platen configuration.

During MBE growth, the platen is rotated, which results in homogeneous growth along a given radius with respect to the center of the platen. To control the homogeneity over the 3” wafers, a stripe alongside the radial direction of the platen is characterized by PL. In Fig. 1 the photon energy and the corresponding peak wavelength of the PL measurement for both superlattices (SL) is depicted as a function of the position on the wafer. Whereas the photon energy measured on the blue diode varies less than ±1 meV, the variation of the red diode with ±2 meV is slightly higher. The corresponding peak wavelength is within ±0.01 μm and ±0.04 μm, respectively. This demonstrates the excellent homogeneity of the T2SL growth over the whole wafer.

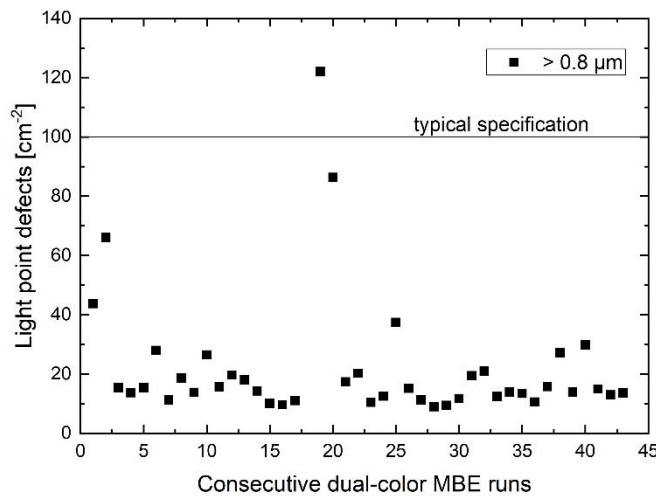


Figure 2. Density of light point defects sized between 0.8 μm and 10 μm measured with a Surfscan 6220 for consecutive growth of dual-color structures with more than 10,000 shutter movements per growth.

Growth defects could deteriorate single or multiple pixels of the detector arrays. Hence, the surface morphology of the epitaxial wafers is intensively monitored. For an automated defect inspection, we use a KLA-Tencor Surfscan 6220. The density of the light point defects (LPD) sized between 0.8  $\mu\text{m}$  and 10  $\mu\text{m}$  for more than 40 consecutive bi-spectral detector structures is plotted in Fig. 2. Despite the fact that there are more than 10,000 shutter movements per dual-color diode structure, most of the growth runs exhibit a LPD density below 20  $\text{cm}^{-2}$ . The defect count for larger defects (not shown here) is negligible.

Much effort has been put in the ability to control the growth rates of InAs and GaSb and achieve a maximum degree of stability and predictability. Finally, an optimization of the cell design was necessary for improved stability of the In and Ga fluxes. With the modified cell design, we established a very stable growth process. In Fig. 3 the period length of both SLs of a bi-spectral detector structure determined by high resolution x-ray diffraction (HRXRD) is shown for more than 40 consecutive growth runs. The standard deviation of the period length for both SLs is merely 0.05 nm. On the right axis of Fig. 3 the approximate sum of the monolayers of GaSb, InAs and InSb is plotted. The offset between the red and the blue SL for the two channels of the bi-spectral detector is only slightly more than a monolayer. For an unambiguous discrimination of hot  $\text{CO}_2$  and thus the functionality of the bi-spectral detector, a sub-monolayer precision is compulsory and has been achieved reproducibly. The PL peak position for the same structures is depicted in Fig. 4. Whereas the period of the SL depends on the InAs and GaSb thickness, the bandgap is mainly determined by the InAs thickness in this structure. For this reason, the PL peak position in Fig. 4 exhibits less variation than the SL period in Fig. 3. For both colors the standard deviation of the PL peak position of consecutive growth runs is around 0.05  $\mu\text{m}$ . Hence, this allows for a cost efficient and reproducible fabrication of sophisticated T2SL detector structures. This would be also true for LWIR and VLWIR structures, as the bandgap is determined by the individual layer thicknesses, which can be controlled as precisely as demonstrated above. In contrast, the fabrication of HgCdTe detectors with good control of the cut-off wavelength is very challenging for longer cut-off wavelengths. The growth of T2SL structures is less sensitive to cut-off wavelength variations and offers very good homogeneity and the potential of scalability to larger formats for higher spatial resolution. In summary, a very stable and reproducible epitaxial growth process has been established. With the mature front- and backside processing reported elsewhere<sup>3-4</sup>, we have set up a pilot line production for bi-spectral detector arrays.

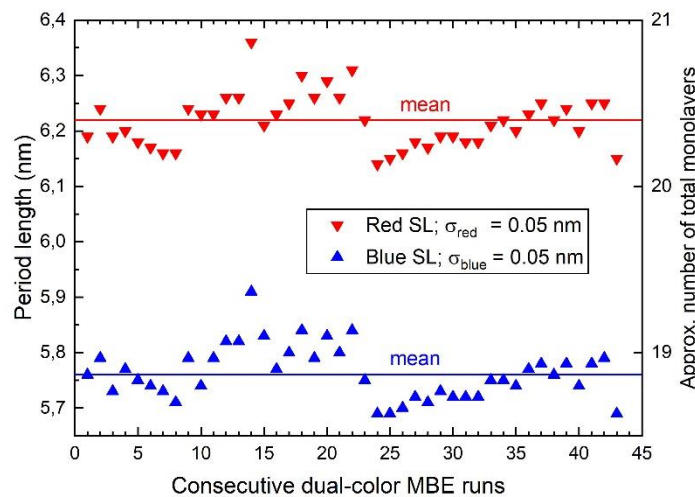


Figure 3. Period lengths of both SLs for consecutive dual color structures. The right axis indicates the approximate sum of the GaSb, InAs and InSb monolayers.

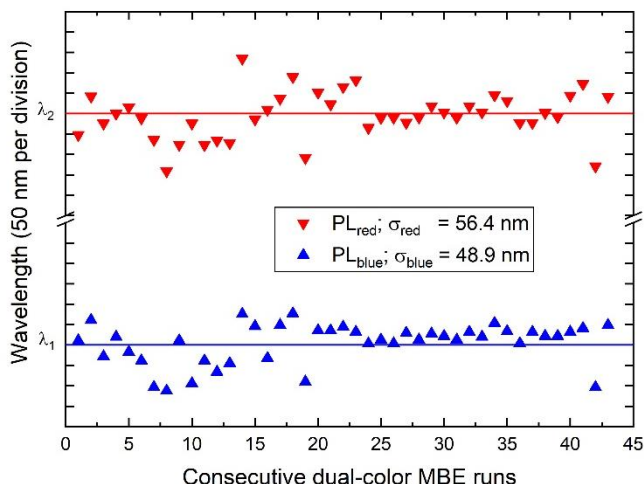


Figure 4. PL peak position for both SLs for consecutively grown dual color layer structures.

### 3. DARK CURRENT MEASUREMENTS

In the beginning the T2SL technology was based on homojunction pin-photodiodes. Meanwhile, heterojunction concepts with unipolar barriers, such as nBn, CBIRD, M-barrier, W-barrier<sup>4-8</sup>, etc., are applied, due to the reduced dark current compared to homojunction photodiodes. We employ a heterojunction device concept by introducing a unipolar barrier consisting of InAs/GaSb SL with different composition and higher bandgap. The band alignment of the barrier and the absorber layer is modelled with the afore mentioned four-component SEPM to ensure conduction band matching. Hence, the photo-generated electrons from the p-type absorber can be unimpededly transported and fully contribute to the photo current without an undesirable onset voltage. The generation-recombination current is suppressed due to the higher bandgap in the barrier layer. Additionally, the valence band offset blocks the transport of the majority holes through the space charge region. We have successfully employed this concept to realize the first T2SL imager for the LWIR with 640×512 pixel and 15 μm pitch in Europe<sup>4</sup>. In the MWIR we have demonstrated the lowest dark currents reported for devices based on InAs/GaSb T2SL absorbers so far<sup>9</sup>.

We have characterized our T2SL detectors down to low temperatures. In Fig. 5 the dark current density at 100 mV reverse bias is plotted in dependence of temperature. The homojunction and heterojunction devices are depicted with open and filled symbols, respectively. For the MWIR (blue) heterojunction devices, the resolution limit of the measurement setup with a dark current density of  $2 \times 10^{-10}$  A/cm<sup>2</sup> has been reached at 77 K. This implies a dark current reduction of more than a factor of 100 compared to an equivalent homojunction device. The LWIR (red) heterojunction devices exhibit a dark current reduction by a factor of 1000 and reach the resolution limit of our measurement setup at 36 K. It is worth noting that the full external quantum efficiency for the heterojunction devices as well as their homojunction counterparts is already obtained at 100 mV. The corresponding dark electrons per second and pixel for a 15 μm pitch is plotted on the right axis. The value of 1000 dark electrons is not suitable for low flux applications, e.g., exoplanet research. However, for high flux applications, e.g., earth observation with relative large number of photons, T2SL detectors offer excellent properties. A comparison with state-of-the-art HgCdTe detectors<sup>10-11</sup>, specially designed for astronomical applications, where low dark currents are required, is shown in Fig. 6. The dark current density is given in dependence of temperature and cut-off wavelength to compare different photodiodes<sup>1</sup>, due to the increase of the cut-off wavelength for HgCdTe with decreasing temperature, which is not the case for T2SLs. Even though our T2SLs were predominantly designed for operating temperatures above 80 K, the dark current density at lower temperatures is already close to the range of HgCdTe detectors. In comparison with HgCdTe diodes, which tend to be limited by tunneling-related dark current components at low temperatures, heterojunction InAs/GaSb T2SL devices suppress tunneling-related dark current components not only with a higher effective carrier mass, but first and foremost with an increased bandgap in the collector superlattice. Hence, InAs/GaSb T2SLs heterojunction devices offer great capabilities for very demanding ultra-low dark current applications, as, e.g., in the field of IR astronomy.

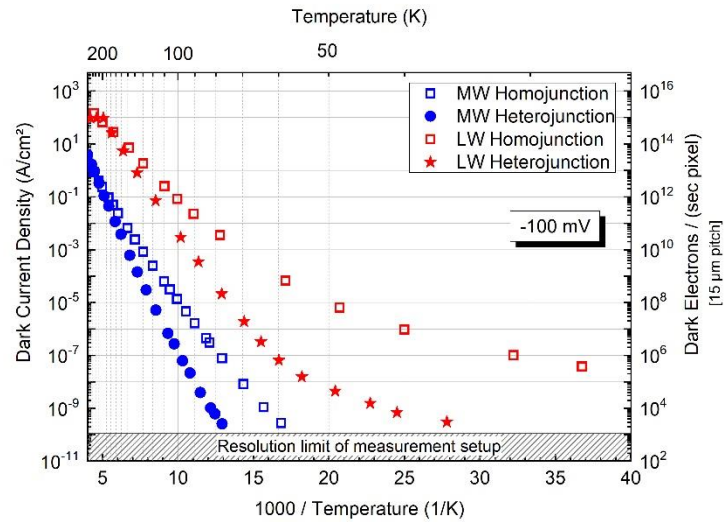


Figure 5. Temperature dependent dark current density of homo- and heterojunction T2SL devices at 100 mV reverse bias. The corresponding number of dark electrons per second per pixel normalized to 15  $\mu\text{m}$  pixels is shown on the right axis.

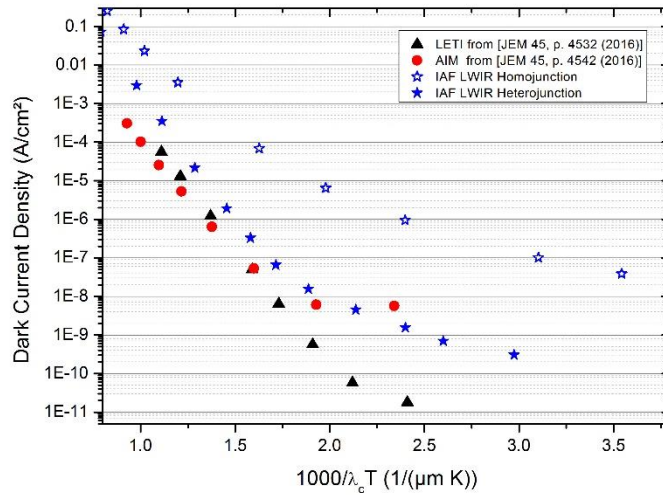


Figure 6. Dark current density of T2SL structures as a function of the inverse temperature and inverse cut-off wavelength in comparison with published HgCdTe data<sup>10-11</sup>.

#### 4. SUMMARY

For the development of T2SL detectors for space applications, Fraunhofer IAF offers a broad spectrum of expertise. We have established validated band structure modelling for the design of high-performance heterojunction devices. With our MBE growth facilities and processing technology we have set up a pilot production line, which provides bi-spectral detector arrays to a procurement program which is at TRL8 on the system level. A wide range of characterization techniques allows for deeper understanding of material properties and the discrimination of failure modes due to material or processing issues. With excellent homogeneity, reproducible growth and processing, and the potential of ultra-low dark current, T2SL technology is a promising candidate for future space applications.

#### ACKNOWLEDGEMENTS

The authors thank S. Fibelkorn, T. Henkel, V. von Hinten, T. Hugger, T. Hultsch, S. Jamil, K. Jung, L. Kirste, N. Kohn, C. Leancu, W. Luppold, M. Prescher and M. Wauro for epitaxy, device processing and characterization and Martin Walther for fruitful discussions. This work has been supported by the German Federal Ministry of Defence and the Bundeswehr Technical Center WTD81 under contract E/E810/EC042/EF039.

#### REFERENCES

- [1] Tennant, W., Lee, D., Zandian, M., Piquette, E., Carmody, M., “MBE HgCdTe Technology: A Very General Solution to IR Detection, Described by “Rule 07”, a Very Convenient Heuristic”, *J. Electron. Mater.* **37**, 1406-1410 (2008).
- [2] Masur, J., Rehm, R., Schmitz, J., Kirste, L., and Walther, M., “Four-component superlattice empirical pseudopotential method for InAs/GaSb superlattices” *Infrared Phys. Technol.* **61**, 129-133 (2013).
- [3] Stadelmann, T., Wörl, A., Wauro, M., Daumer, V., Niemasz, J., Luppold, W., Simon, T., Riedel, M., Rehm, R., and Walther, M., “Development of bi-spectral InAs/GaSb type II superlattice image detectors” *Proc. SPIE* **9070**, 90700V (2014).
- [4] Rehm, R., Daumer, V., Hugger, T., Kohn, N., Luppold, W., Mueller, R., Niemasz, J., Schmidt, J., Rutz, F., Stadelmann, T., Wauro, M., Woerl, A., “Type-II Superlattice Infrared Detector Technology at Fraunhofer IAF” *Proc. SPIE* **9819**, 98190X (2016).
- [5] Ting, D.Z.Y., Hill, C.J., Soibel, A., Keo, S.A., Mumolo, J.M., Nguyen, J., Gunapala, S.D., “A high-performance long wavelength superlattice complementary barrier infrared detector”, *Appl. Phys. Lett.* **95** (2009) 023508.
- [6] Vurgaftman, I., Aifer, E.H., Canedy, C.L., Tischler, J.G., Meyer, J.R., Warner, J.H., Jackson, E.M., Hildebrandt, G., Sullivan, G.J., “Graded band gap for dark-current suppression in long-wave infrared W-structured type-II superlattice photodiodes”, *Appl. Phys. Lett.* **89** (2006) 121114.
- [7] Nguyen, B.-M., Hoffman, D., Delaunay, P.-Y., Razeghi, M., “Dark current suppression in type II InAs/GaSb superlattice long wavelength infrared photodiodes with M-structure barrier”, *Appl. Phys. Lett.* **91** (2007) 163511.
- [8] Rodriguez, J.B., Plis, E., Bishop, G., Sharma, Y.D., Kim, H., Dawson, L.R., Krishna, S., “NBn structure based on InAs/GaSb type-II strained layer superlattices”, *Appl. Phys. Lett.* **91** (2007) 043514.
- [9] Schmidt, J., Rutz, F., Woerl, A., Daumer, V., Rehm, R., „Low dark current in mid-infrared type-II superlattice heterojunction photodiodes”, *Infrared Phys. Technol.* **85**, 378-381 (2017)
- [10] Gravrand, O., Rothman, J., Cervera, C., Baier, N., Lobre, C., Zanatta, J.P., Boulade, O., Moreau, V., Fieque, B., “HgCdTe Detectors for Space and Science Imaging: General Issues and Latest Achievements”, *J. Electron. Mater.* **45**, 4532-4541 (2016).
- [11] Hanna, S., Eich, D., Mahlein, K.-M., Fick, W., Schirmacher, W., Thöt, R., Wendler, J., Figgemeier, H., “MCT-Based LWIR and VLWIR 2D Focal Plane Detector Arrays for Low Dark Current Applications at AIM”, *J. Electron. Mater.* **45**, 4542-4551 (2016).